Cell Reports Medicine, Volume *4*

Supplemental information

Multiplex immune profiling reveals the role of serum immune proteomics in predicting response to preoperative chemotherapy of gastric cancer

Zhaoqing Tang, Yuan Gu, Zhongyi Shi, Lingqiang Min, Ziwei Zhang, Peng Zhou, Rongkui Luo, Yan Wang, Yuehong Cui, Yihong Sun, and Xuefei Wang

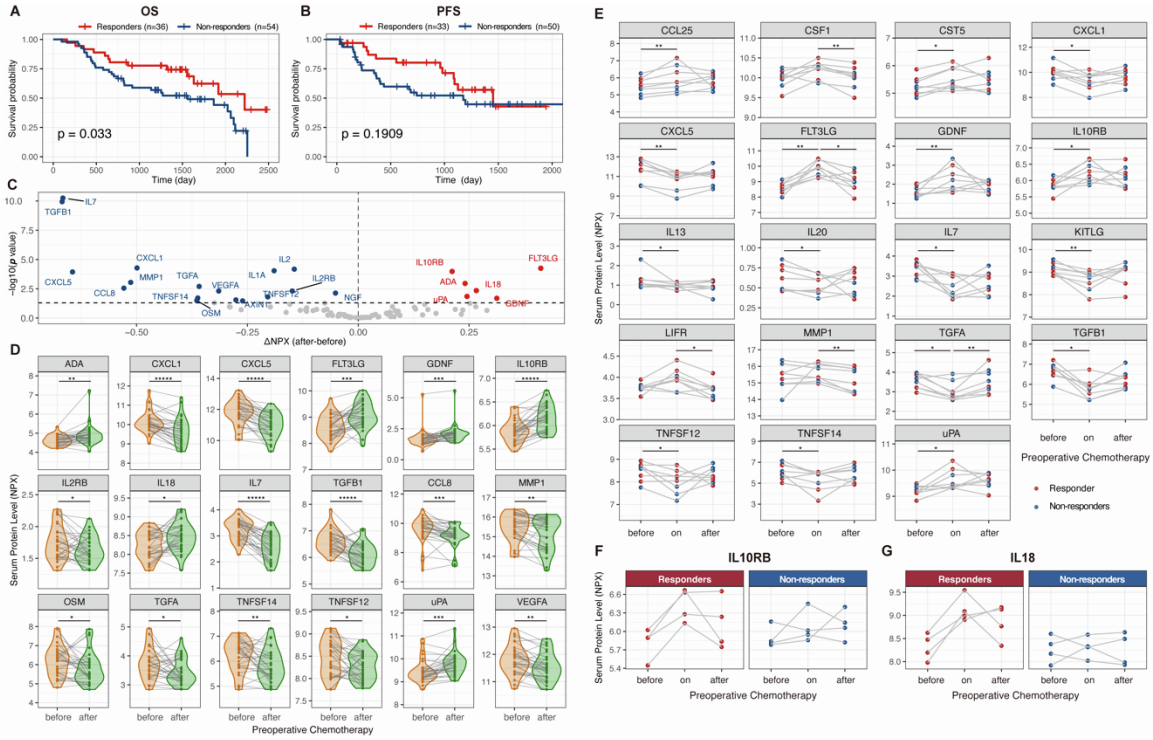

Figure S1. Dynamics of serum immune proteomics during and after preoperative chemotherapy, related to Figure 1. (A). Kaplan–Meier curves of overall survival (OS) for patients with different treatment responses. Log-rank test showed *p*=0.033. (B) Kaplan–Meier curves of progression-free survival (PFS) for patients with different treatment responses. Log-rank test showed *p*=0.1909. (C) Volcano plot showed serum proteins whose levels changed after preoperative chemotherapy in unpaired tests (before n=37, after n=83). (D) The dynamics of the serum proteins showing a significant change after preoperative chemotherapy in both paired and unpaired tests. Only paired serum samples were shown. (E) Dynamics of serum proteins showing a significant change during preoperative chemotherapy. (F) Dynamics of serum IL10RB level during preoperative chemotherapy in responders and non-responders. (G) Dynamics of serum IL18 level during preoperative chemotherapy in responders and non-responders.

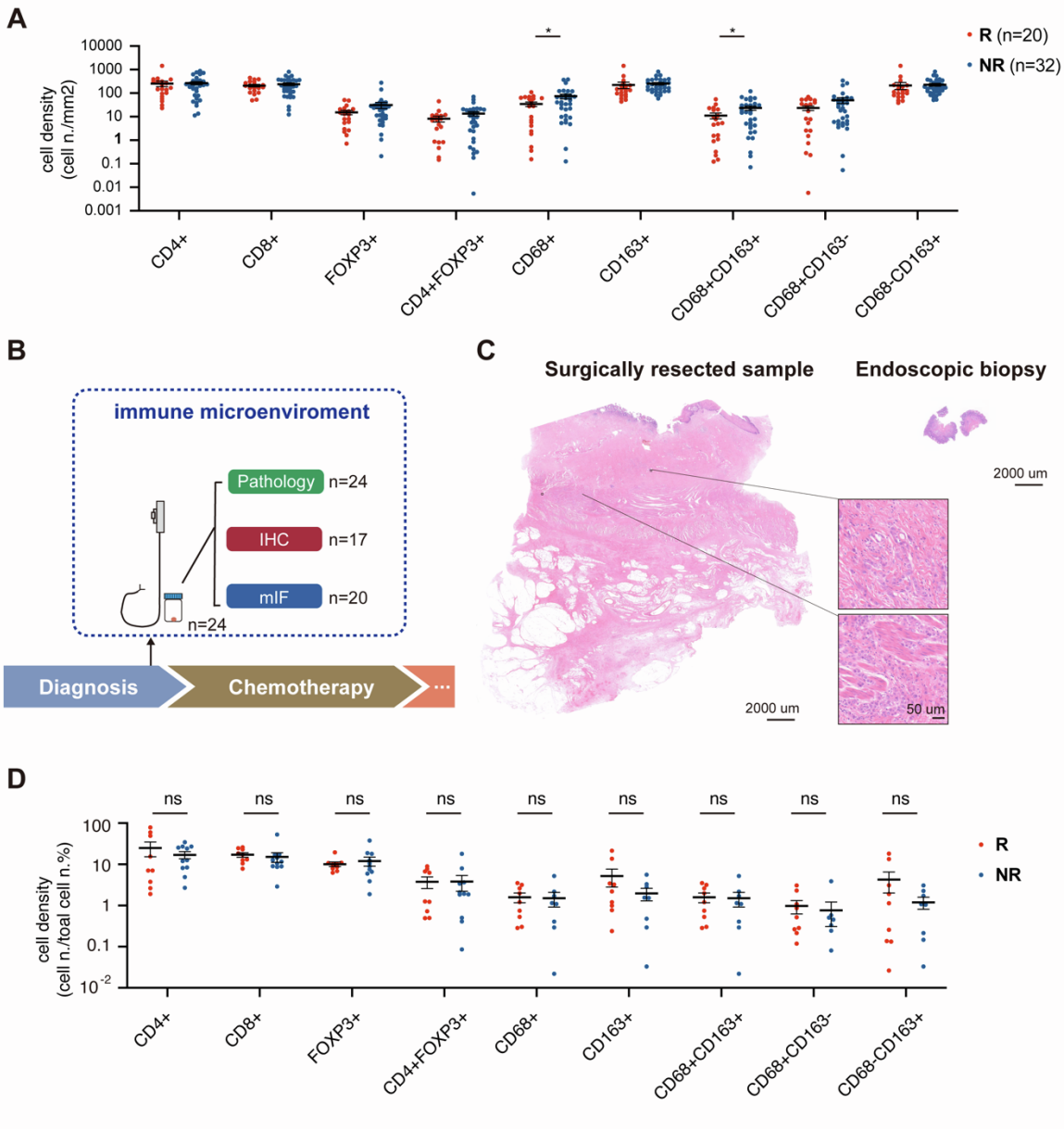

Figure S2. Pretreatment TME features based on endoscopic biopsy, related to Figure 2.

(A) Comparison of immune cell infiltration in post-treatment tumor samples in patients with different treatment responses (responder n=20; non-responder n=32). Cell density calculated by positive cell numbers/area(mm^2). (B) Flow chart of endoscopic biopsy sample collection (C) Representative images of surgically resected samples and endoscopic biopsies. (D) Comparison of immune cell infiltration in pretreatment endoscopic biopsy samples from patients with different treatment responses (responder n=9; non-responder n=11). Cell density calculated by positive cell numbers/total cell numbers.

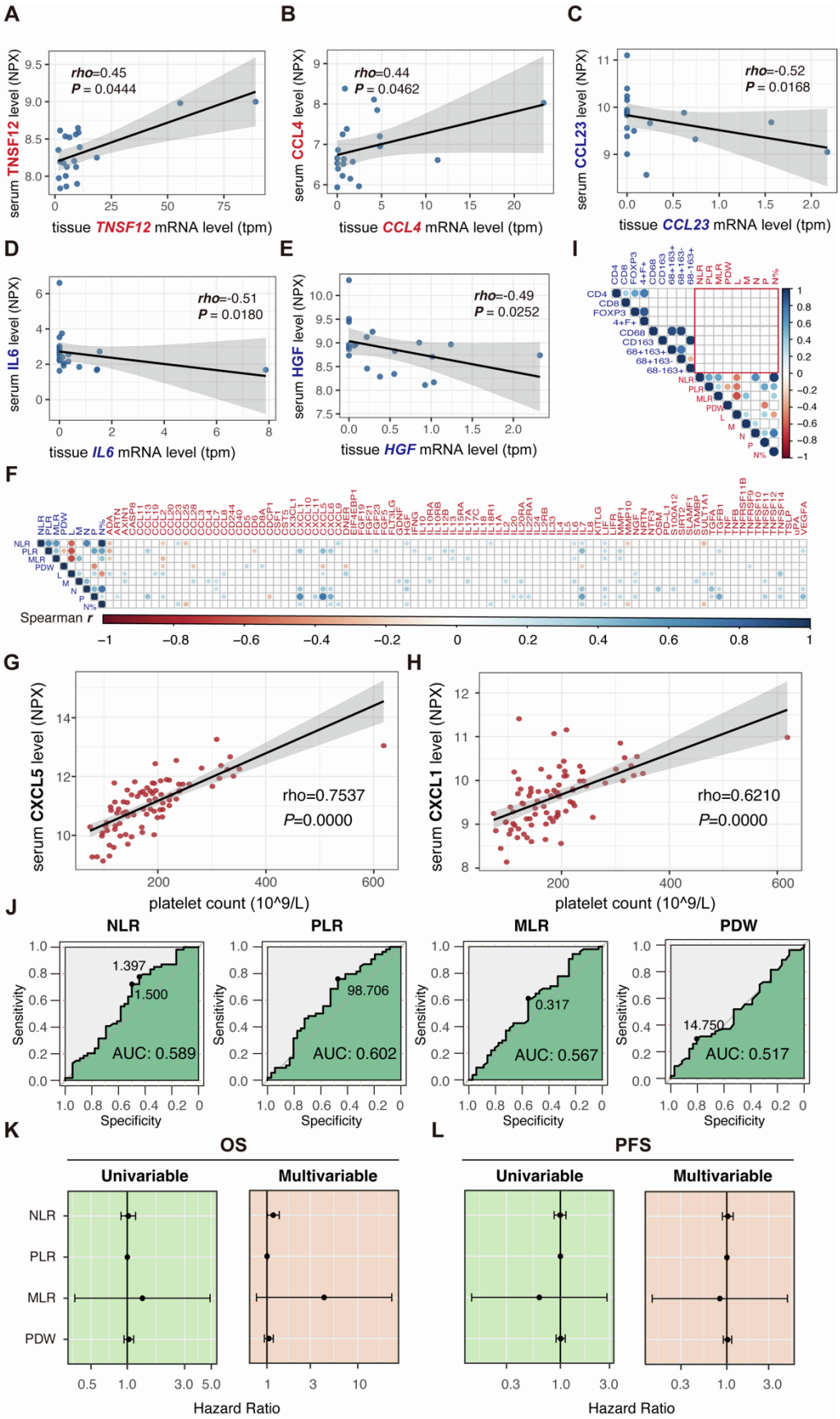
A
serum TNSF12 level (NPX)
rho=0.45
P = 0.0444
tissue TNSF12 mRNA level (tpm)
B
serum CCL4 level (NPX)
rho=0.44
P = 0.0462
tissue CCL4 mRNA level (tpm)
C
serum CCL23 level (NPX)
rho=-0.52
P = 0.0168
tissue CCL23 mRNA level (tpm)
D
serum IL6 level (NPX)
rho=-0.51
P = 0.0180
tissue IL6 mRNA level (tpm)
E
serum HGF level (NPX)
rho=-0.49
P = 0.0252
tissue HGF mRNA level (tpm)
I
F
Spearman r
G
serum CXCL5 level (NPX)
rho=0.7537
P=0.0000
platelet count (10^9/L)
H
serum CXCL1 level (NPX)
rho=0.6210
P=0.0000
platelet count (10^9/L)
J
NLR
PLR
MLR
PDW
Sensitivity
Specificity
1.397
1.500
AUC: 0.589
98.706
AUC: 0.602
0.317
AUC: 0.567
14.750
AUC: 0.517
K
OS
Univariable
Multivariable
NLR
PLR
MLR
PDW
Hazard Ratio
L
PFS
Univariable
Multivariable
Hazard Ratio

Figure S3. Correlations between local and systemic immune features and clinical value of classic systemic immune-inflammation indices, related to Figure 3. (A) Correlation between post-treatment serum TNSF12 level and tissue *TNF12* mRNA level. (B) Correlation between post-treatment serum CCL4 level and tissue *CCL4* mRNA level. (C) Correlation between post-treatment serum CCL23 level and tissue *CCL23* mRNA level. (D) Correlation between post-treatment serum IL6 level and tissue *IL6* mRNA level. (E) Correlation between post-treatment serum HGF level and tissue *HGF* mRNA level. The *rho* values and *p* values of Spearman's correlation were indicated. (F) Correlations between post-treatment serum proteomics and four immune-inflammation indices, and common blood cell counts. *Rho* values of correlations with *p* value<0.05 were indicated by different colors as indicated (G) Correlation between post-treatment serum CXCL5 level and peripheral blood platelet count. (H) Correlation between post-treatment serum CXCL1 level and peripheral blood platelet count. *Rho* and *p* values of Spearman correlation as indicated. (I) Correlations between classic systemic immune-inflammation indices and immune cell infiltration in TME. The rho values of correlations with *p* value<0.05 were indicated by different colors as indicated. (J) ROC curve demonstrating treatment response predictive accuracy of four classic systemic immune-inflammation indices. (K) Hazard ratio (HR) of four classic systemic immune-inflammation indices for overall survival (OS) calculated by univariable/multivariable cox regression. (L) Hazard ratio (HR) of four classic systemic immune-inflammation indices for progression-free survival (PFS) calculated by univariable/ multivariable cox regression.

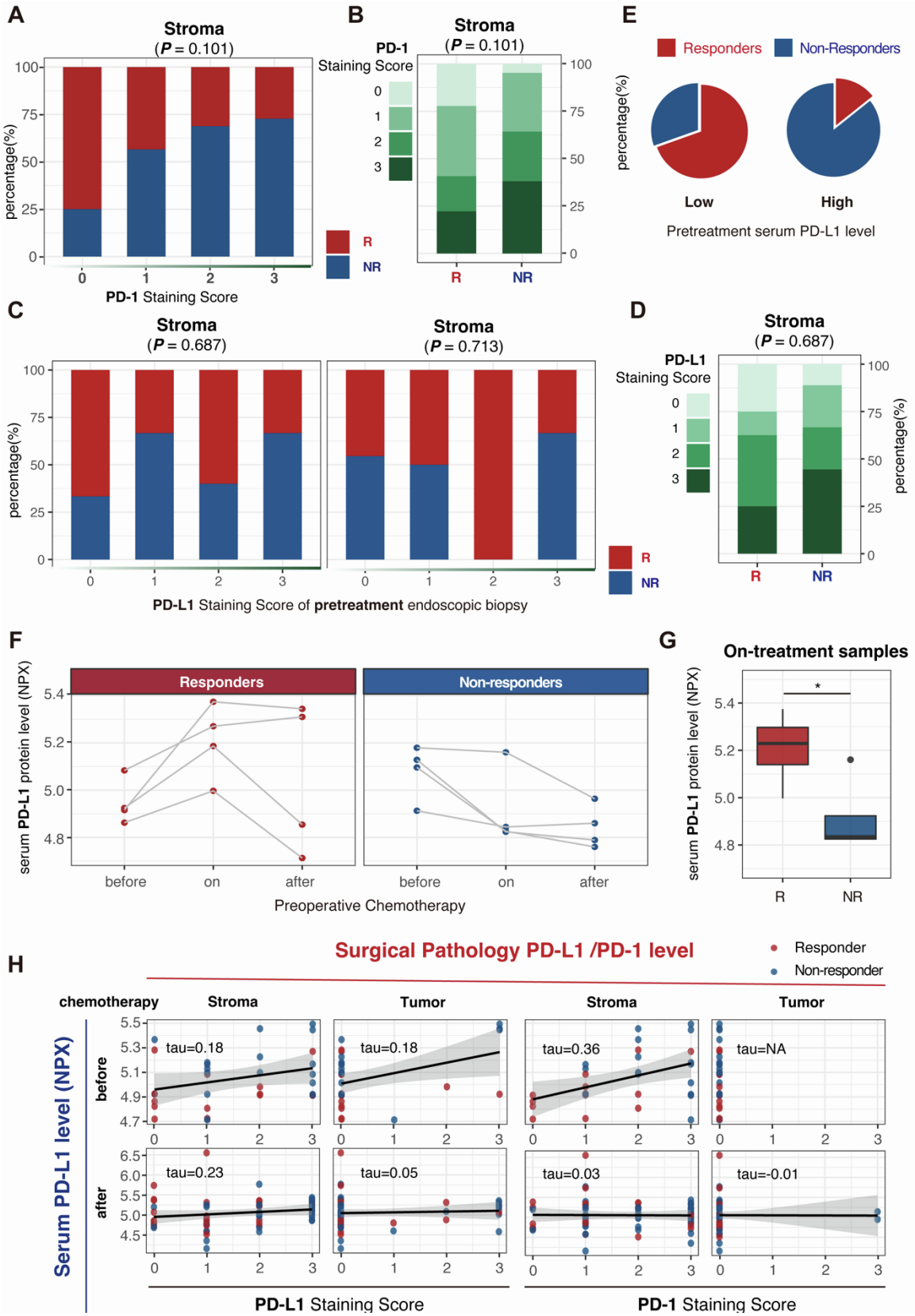

Figure S4. Correlation between tissue PD1/PD-L1 staining and serum PD-L1 level, and their

associations with treatment response, related to Figure 4. (A) Treatment response in patients (n=70) with different stromal PD-1 staining scores. (B) Stromal PD-1 staining scores in patients with different treatment response (responders n=33, non-responders n=50). (C) Treatment response in patients (n=17) with different stromal/tumor PD-L1 staining scores of their pretreatment endoscopic biopsies. (D) Pretreatment stromal PD-L1 staining scores of patients with different treatment responses. (E) Treatment responses in patients with high (>5.084 NPX, n=14) and low (<5.084 NPX, n=23) pretreatment serum PD-L1 level. (F) Dynamics of serum PD-L1 level during preoperative chemotherapy. (G) On-treatment serum PD-L1 level differed in patients with different responses. (H) Correlation between surgical pathology PD-L1 /PD-1 level and serum PD-L1 level. *Tau* values of Kendall rank correlation were indicated.

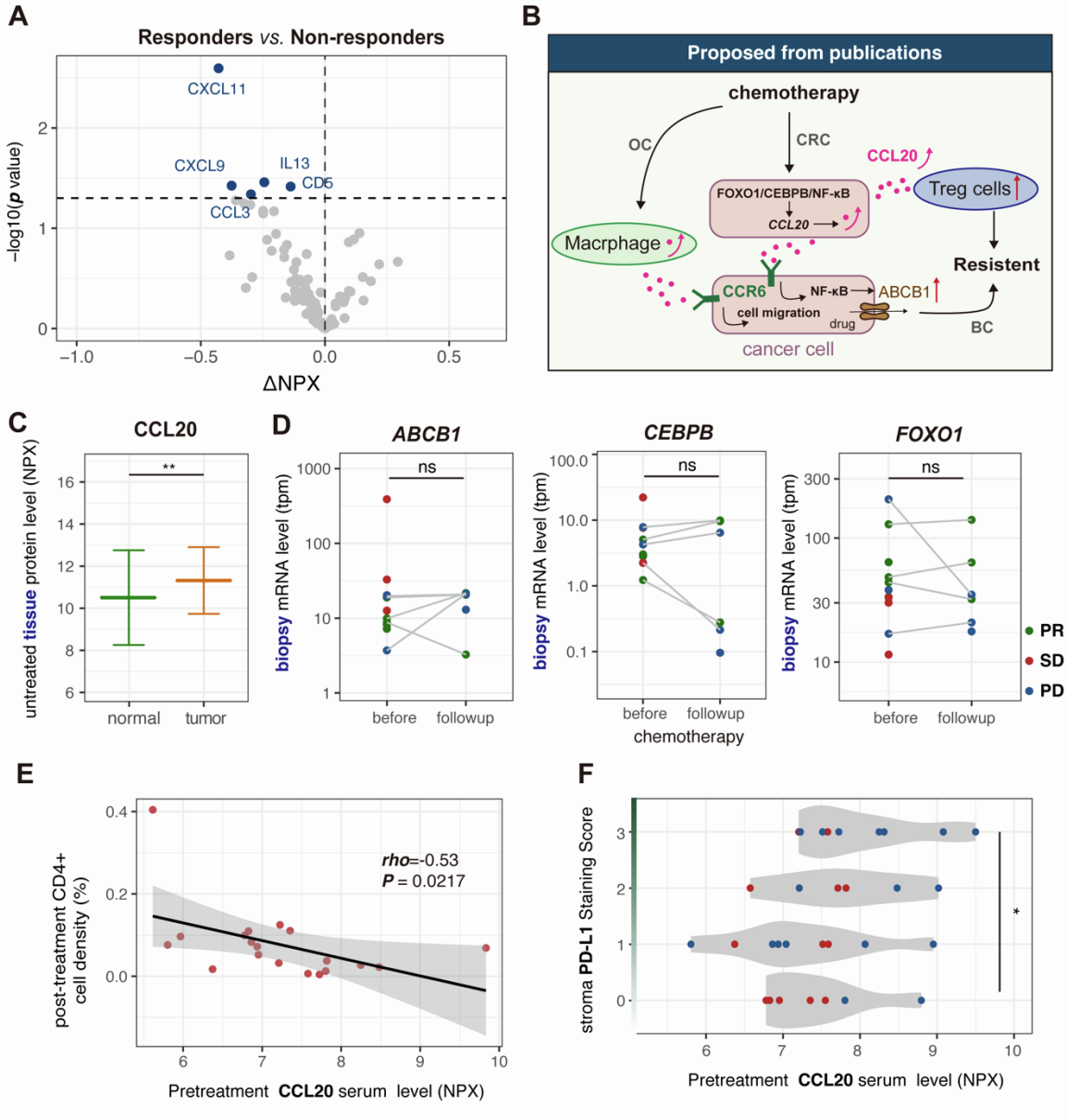

Figure S5. Potential role of CCL20 in chemoresistance, related to Figure 5. (A) Comparison of post-treatment serum protein levels in responders and non-responders. (B) Mechanisms of *CCL20* upregulation reported in breast cancer (BC), ovarian cancer (OC), and colorectal cancer (CRC). (C) Gastric tumor had higher CCL20 protein level compared with normal gastric tissues. (D) Biopsy tumor sample showed no change in *ABCB*, *CEBPB*, and *FOXO1* mRNA level before and during treatment in patients with gastric cancer undergoing first-line standard chemotherapy. (E) Higher pretreatment CCL20 level was linked to less CD4(+) T cell infiltration in post-treatment tumors. (F) Higher pretreatment CCL20 level was linked to higher stromal PD-L1 staining in post-treatment tumors.

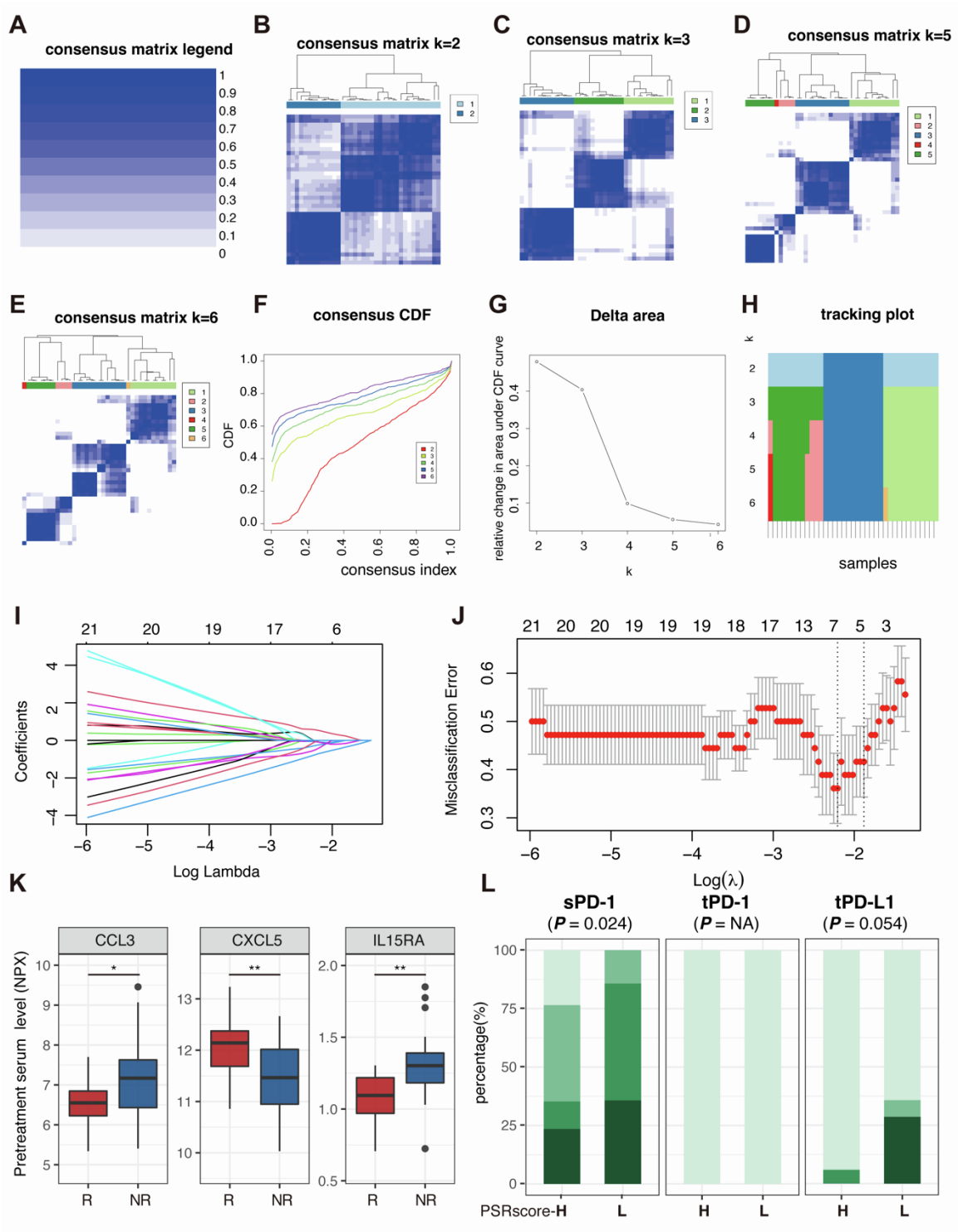

Figure S6. Unsupervised consensus clustering and LASSO model of pretreatment serum proteomics, related to Figure 6. (A -E) Consensus matrix heat maps based on the number of clusters (from k=2 to 6). (F) Cumulative distribution function (CDF) under corresponding k values. (G) Relative change in area (delta area) under the cumulative distribution function (CDF) curves when the cluster number varies from k=2 to 6. (H) Sample clustering under different k values. (I) Average error and standard deviation over the folds after

k-fold cross-validation in LASSO model. (J) Misclassification error in different λ value. A λ value= 0.16 with log (λ) = -1.834 was chosen by cross-validation via the 1-SE criteria. (K) Responders (n=18) had lower serum CCL3 and IL15RA level and higher CXCL5 level before chemotherapy compared with non-responders (n=19). (L) Post-treatment stromal PD-1 level and tumor PD-1/PD-L1 level in patients with high/low PSRscores (H: n=18, L: n=14).

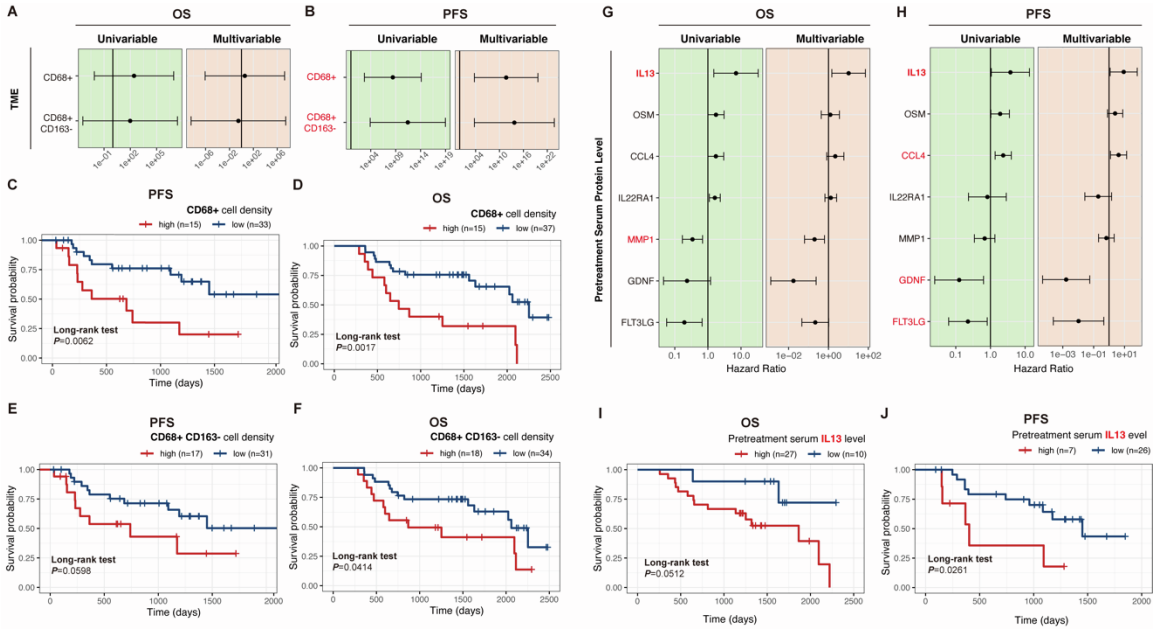

Figure S7. Prognostic value of immune cell infiltration in TME and pretreatment serum proteomics, related to Figure 7. (A) Hazard ratios (HR) of different immune cell infiltration in TME for overall survival calculated by univariable/ multivariable cox regression. (B) HR of different immune cell infiltration in TME for progression-free survival calculated by univariable/ multivariable cox regression. The length of the horizontal line represented the 95% confidence interval of HR for each protein. The vertical solid line represented HR= 1. (C) Kaplan–Meier curves of PFS for patients with high (n=15) and low (n=33) CD68(+) cell infiltration. (D) Kaplan–Meier curves of OS for patients with high (n=15) and low (n=37) CD68(+) cell infiltration. (E) Kaplan–Meier curves of PFS for patients with high (n=17) and low (n=31) CD68(+) and CD163(-) cell infiltration. (F) Kaplan–Meier curves of OS for patients with high (n=18) and low (n=34) CD68(+) and CD163(-) cell infiltration. The *p* value of Log-rank test and HR of multivariable cox regression were indicated. (G) Hazard ratios (HR) of pretreatment serum protein levels for overall survival calculated by univariable/ multivariable cox regression. (H) HR of post-treatment serum protein levels for progression-free survival calculated by univariable/ multivariable cox regression. The length of the horizontal line represented the 95% confidence interval of HR for each protein. The vertical solid line represented HR= 1. (I) Kaplan–Meier curves of overall survival (OS) for patients with high (n=27) and low (n=10) post-treatment serum IL13 level. (J) Kaplan–Meier curves of progression-free survival (PFS) for patients with high (n=7) and low (n=26) post-treatment serum IL13 level. The *p* value of Log-rank test and HR of multivariable cox regression were indicated.

Tables

Table S1. Clinical characteristics of patients, related to Figure 7.

Response	Good	Poor	Total	*P* value
N	36	54	90	
gender = M (%)	26 (72.2)	42 (77.8)	68 (75.6)	0.726
age = >=60 (%)	19 (52.8)	32 (59.3)	51 (56.7)	0.696
location = non-AEJ (%)	31 (86.1)	39 (72.2)	70 (77.8)	0.196
Lauren (%)				0.846
diffuse	9 (25.0)	14 (25.9)	23 (25.6)	
Intestinal	15 (41.7)	25 (46.3)	40 (44.4)	
mixed	12 (33.3)	15 (27.8)	27 (30.0)	
differentiation (%)				0.083
G2	11 (30.6)	8 (14.8)	19 (21.1)	
G3	24 (66.7)	46 (85.2)	70 (77.8)	
Gx	1 (2.8)	0 (0.0)	1 (1.1)	
regimens (%)				0.167
Two-drug	14 (38.9)	29 (53.7)	43 (47.8)	
Three-drug	21 (58.3)	21 (38.9)	42 (46.7)	
Other	1 (2.8)	4 (7.4)	5 (5.6)	
ypT (%)				0.312
1a	2 (5.6)	1 (1.9)	3 (3.3)	
1b	3 (8.3)	1 (1.9)	4 (4.4)	
2	10 (27.8)	12 (22.2)	22 (24.4)	
3	11 (30.6)	20 (37.0)	31 (34.4)	
4a	9 (25.0)	20 (37.0)	29 (32.2)	
X	1 (2.8)	0 (0.0)	1 (1.1)	
ypN (%)				<0.001
0	19 (52.8)	8 (14.8)	27 (30.0)	
1	11 (30.6)	10 (18.5)	21 (23.3)	
2	0 (0.0)	15 (27.8)	15 (16.7)	
3a	6 (16.7)	9 (16.7)	15 (16.7)	
3b	0 (0.0)	12 (22.2)	12 (13.3)	
ypM = 1 (%)	13 (36.1)	13 (24.1)	26 (28.9)	0.319
ypTNM (%)				0.021
I	9 (25.0)	5 (9.3)	14 (15.6)	
II	7 (19.4)	11 (20.4)	18 (20.0)	
III	6 (16.7)	25 (46.3)	31 (34.4)	
IV	13 (36.1)	13 (24.1)	26 (28.9)	
Other	1 (2.8)	0 (0.0)	1 (1.1)	
LVI = Positive (%)	10 (27.8)	31 (57.4)	41 (45.6)	0.011

PNI = Positive (%)	18 (50.0)	35 (64.8)	53 (58.9)	0.238

Table S2. Multivariate survival analysis of serum post-treatment IL10RB level based on OS, related to Figure 7.

	univariable cox regression			multivariable cox regression		
Characteristics	**Hazard ratio (95% CI)**	***P* value**		**Hazard ratio (95% CI)**	***P* value**	
gender = M	0.7146 (0.3791, 1.347)	0.299		1.407 (0.5225, 3.769)	0.497	
age = >=60	0.704 (0.3885, 1.276)	0.247		0.5613 (0.2468, 1.277)	0.168	
location= non-AEJ	1.671 (0.7454, 3.745)	0.213				
Lauren						
diffuse	reference			Reference		
Intestinal	0.3014 (0.1458, 0.6232)	0.001	**	0.4279 (0.1498, 1.222)	0.113	
mixed	0.5435 (0.2708, 1.0909)	0.086	.	0.6309 (0.2337, 1.703)	0.363	
differentiation						
G2	reference			Reference		
G3	4.438 (1.3675, 14.4)	0.013	*	1.54 (0.3791, 6.259)	0.546	
Gx	6.936 (0.7154, 67.24)	0.095	.	1.385 (0.1084, 17.697)	0.802	
regimens (%)						
Other	reference					
Two-drug	1.232 (0.3591, 4.227)	0.740				
Three-drug	1.536 (0.4475, 5.272)	0.495				
ypTNM						
I	reference			Reference		
II	2.522 (0.5074, 12.54)	0.258		3.053 (0.3335, 27.95)	0.323	
III	6.08 (1.4182, 26.07)	0.015	*	5.332 (0.6065, 46.873)	0.131	
IV	6.259 (1.4427, 27.15)	0.014	*	10.08 (1.2552, 80.883)	0.030	*
Other	0 (0, Inf)	0.997		0 (0, Inf)	0.998	
LVI = Positive	2.867 (1.524, 5.391)	0.001	**	1.996 (0.9191, 4.334)	0.081	.
PNI = Positive	2.033 (1.062, 3.892)	0.032	*	1.431 (0.6281, 3.262)	0.393	
IL10RB level	3.086 (1.055, 9.031)	0.040	*	5.622 (1.7884, 17.676)	0.003	**

Table S3. Multivariable cox regression of post-treatment serum IL10RB level based on PFS, related to Figure 7.

	univariable cox regression			multivariable cox regression		
Characteristics	**Hazard ratio (95% CI)**	***P* value**		**Hazard ratio (95% CI)**	***P* value**	
gender = M	0.8883 (0.4025, 1.961)	0.769		1.109 (0.3878,3.173)	0.846	
age = >=60	0.7027 (0.3619,1.364)	0.297		0.491 (0.2101,1.147)	0.100	
location= non-AEJ	1.507 (0.5844,3.884)	0.396				
Lauren						
diffuse	reference			reference		
Intestinal	0.3920 (0.1725,0.8907)	0.0253	*	0.8374 (0.2711,2.587)	0.758	
mixed	0.8524 (0.3821,1.9015)	0.6964		1.484 (0.4185,5.261)	0.541	
differentiation						
G2	reference					
G3	2.2569 (0.8714,5.846)	0.0937	.			
Gx	3.104 (0.3609,26.693)	0.3022				
regimens (%)						
other	reference					
Two-drug	1.483 (0.1980,11.1)	0.701				
Three-drug	1.369 (0.1803,10.39)	0.761				
ypTNM						
I	reference			reference		
II	1.290 (0.3634,4.581)	0.693		1.702 (0.3868,7.489)	0.482	
III	2.402 (0.7942,7.267)	0.121		3.566 (0.7414,17.152)	0.113	
IV	2.211 (0.6925,7.06)	0.180		4.816 (1.1227,20.654)	0.034	*
other	0 (0,Inf)	0.997		0 (0,Inf)	0.997	
LVI = Positive	1.978 (1.008 ,3.884)	0.0474	*	1.529 (0.61,3.832)	0.365	
PNI = Positive	2.782 (1.262,6.135)	0.0112	*	3.464 (1.2484,9.61)	0.017	*
IL10RB level	4.3918 (1.185,16.27)	0.0268	*	14.35 (3.0624,67.216)	0.001	***

Table S4. Proteins included in Olink proteomics Target 96 inflammation panel, related to serum immune proteomics in STAR Methods.

UniprotID	Protein name	abbrevation
O00300	Osteoprotegerin (OPG)	TNFRSF1 1B
O14625	C-X-C motif chemokine 11 (CXCL11)	CXCL11
O14788	TNF-related activation-induced cytokine (TRANCE)	TNFSF11
O15169	Axin-1 (AXIN1)	AXIN1
O15444	C-C motif chemokine 25 (CCL25)	CCL25
O43508	Tumor necrosis factor (Ligand) superfamily, member 12 (TWEAK)	TNFSF12
O43557	Tumor necrosis factor ligand superfamily member 14 (TNFSF14)	TNFSF14
O95630	STAM-binding protein (STAMPB)	STAMBP
O95750	Fibroblast growth factor 19 (FGF-19)	FGF19
O95760	Interleukin-33 (IL-33)	IL33
P00749	Urokinase-type plasminogen activator (uPA)	uPA
P00813	Adenosine Deaminase (ADA)	ADA
P01135	Transforming growth factor alpha (TGF-alpha)	TGFA
P01137	Latency-associated peptide transforming growth factor beta-1 (LAP TGF-beta-1)	TGFB1
P01138	Beta-nerve growth factor (Beta-NGF)	NGF
P01374	TNF-beta (TNFB)	TNFB
P01375	Tumor necrosis factor (TNF)	TNF
P01579	Interferon gamma (IFN-gamma)	IFNG
P01583	Interleukin-1 alpha (IL-1 alpha)	IL1A
P01732	T-cell surface glycoprotein CD8 alpha chain (CD8A)	CD8A
P02778	C-X-C motif chemokine 10 (CXCL10)	CXCL10
P03956	Matrix metalloproteinase-1 (MMP-1)	MMP1
P05112	Interleukin-4 (IL-4)	IL4
P05113	Interleukin-5 (IL5)	IL5
P05231	Interleukin-6 (IL6)	IL6
P06127	T-cell surface glycoprotein CD5 (CD5)	CD5
P09238	Matrix metalloproteinase-10 (MMP-10)	MMP10
P09341	C-X-C motif chemokine 1 (CXCL1)	CXCL1
P09603	Macrophage colony-stimulating factor 1 (CSF-1)	CSF1
P10145	Interleukin-8 (IL-8)	IL8
P10147	C-C motif chemokine 3 (CCL3)	CCL3
P12034	Fibroblast growth factor 5 (FGF-5)	FGF5
P13232	Interleukin-7 (IL-7)	IL7
P13236	C-C motif chemokine 4 (CCL4)	CCL4
P13500	Monocyte chemotactic protein 1 (MCP-1)	CCL2
P13725	Oncostatin-M (OSM)	OSM
P14210	Hepatocyte growth factor (HGF)	HGF
P14784	Interleukin-2 receptor subunit beta (IL-2RB)	IL2RB

P15018	Leukemia inhibitory factor (LIF)	LIF
P15692	Vascular endothelial growth factor A (VEGF-A)	VEGFA
P20783	Neurotrophin-3 (NT-3)	NTF3
P21583	Stem cell factor (SCF)	KITLG
P22301	Interleukin-10 (IL10)	IL10
P25942	CD40L receptor (CD40)	CD40
P28325	Cystatin D (CST5)	CST5
P29460	Interleukin-12 subunit beta (IL-12B)	IL12B
P30203	T cell surface glycoprotein CD6 isoform (CD6)	CD6
P35225	Interleukin-13 (IL-13)	IL13
P39905	Glial cell line-derived neurotrophic factor (GDNF)	GDNF
P42702	Leukemia inhibitory factor receptor (LIF-R)	LIFR
P42830	C-X-C motif chemokine 5 (CXCL5)	CXCL5
P49771	Fms-related tyrosine kinase 3 ligand (Flt3L)	FLT3LG
P50225	Sulfotransferase 1A1 (ST1A1)	SULT1A1
P50591	TNF-related apoptosis-inducing ligand (TRAIL)	TNFSF10
P51671	Eotaxin (CCL11)	CCL11
P55773	C-C motif chemokine 23 (CCL23)	CCL23
P60568	Interleukin-2 (IL-2)	IL2
P78423	Fractalkine (CX3CL1)	CX3CL1
P78556	C-C motif chemokine 20 (CCL20)	CCL20
P80075	Monocyte chemotactic protein 2 (MCP-2)	CCL8
P80098	Monocyte chemotactic protein 3 (MCP-3)	CCL7
P80162	C-X-C motif chemokine 6 (CXCL6)	CXCL6
P80511	Protein S100-A12 (EN-RAGE)	S100A12
Q07011	Tumor necrosis factor receptor superfamily member 9 (TNFRSF9)	TNFRSF9
Q07325	C-X-C motif chemokine 9 (CXCL9)	CXCL9
Q08334	Interleukin-10 receptor subunit beta (IL-10RB)	IL10RB
Q13007	Interleukin-24 (IL-24)	IL24
Q13261	Interleukin-15 receptor subunit alpha (IL-15RA)	IL15RA
Q13291	Signaling lymphocytic activation molecule (SLAMF1)	SLAMF1
Q13478	Interleukin-18 receptor 1 (IL-18R1)	IL18R1
Q13541	Eukaryotic translation initiation factor 4E-binding protein 1 (4E-BP1)	EIF4EBP1
Q13651	Interleukin-10 receptor subunit alpha (IL-10RA)	IL10RA
Q14116	Interleukin-18 (IL-18)	IL18
Q14790	Caspase-8 (CASP-8)	CASP8
Q16552	Interleukin-17A (IL-17A)	IL17A
Q5T4W7	Artemin (ARTN)	ARTN
Q8IXJ6	SIR2-like protein 2 (SIRT2)	SIRT2
Q8N6P7	Interleukin-22 receptor subunit alpha-1 (IL-22 RA1)	IL22RA1
Q8NFT8	Delta and Notch-like epidermal growth factor-related receptor (DNER)	DNER

Q969D9	Thymic stromal lymphopoietin (TSLP)	TSLP
Q99616	Monocyte chemotactic protein 4 (MCP-4)	CCL13
Q99731	C-C motif chemokine 19 (CCL19)	CCL19
Q99748	Neurturin (NRTN)	NRTN
Q9BZW8	Natural killer cell receptor 2B4 (CD244)	CD244
Q9GZV9	Fibroblast growth factor 23 (FGF-23)	FGF23
Q9H5V8	CUB domain-containing protein 1 (CDCP1)	CDCP1
Q9NRJ3	C-C motif chemokine 28 (CCL28)	CCL28
Q9NSA1	Fibroblast growth factor 21 (FGF-21)	FGF21
Q9NYY1	Interleukin-20 (IL-20)	IL20
Q9NZQ7	Programmed cell death 1 ligand 1 (PD-L1)	PD-L1
Q9P0M4	Interleukin-17C (IL-17C)	IL17C
Q9UHF4	Interleukin-20 receptor subunit alpha (IL-20RA)	IL20RA